micromachines

MDPI

Article

Optimizing Broadband Near-Infrared Emission in Bi/Sn-Doped Aluminosilicate Glass by Modulating Glass Composition

Song Xiang [1], Min Zhang [1,*], Tixian Zeng [2], Jiang Chen [3] and Feiquan Zhang [3]

[1] School of Physics and Astronomy, China West Normal University, Nanchong 637002, China; xiangsong@stu.cwnu.edu.cn
[2] College of Optoelectronic Engineering, Chengdu University of Information Technology, Chengdu 610225, China; zengtxnc@163.com
[3] Sichuan Hetai Optical Fiber Co., Ltd., Nanchong 637002, China; chenjiang985464@163.com (J.C.); zhangfeiquan2022@163.com (F.Z.)
* Correspondence: zmzmi1987@163.com; Tel./Fax: +86-0817-2568348

Abstract: The Bi/Sn-doped aluminosilicate glass samples were prepared using a melting–quenching method and their near-infrared (NIR) emission properties were studied. An ultra-broadband NIR emission ranging from 950 nm to 1600 nm was observed in all samples under 480 nm excitation, which covered the whole fiber low-loss window. The NIR emission spectrum showed that the maximum emission peak was about 1206 nm and the full width at half maximum (FWHM) was about 220 nm. Furthermore, the NIR emission intensity strongly depends on the composition of the glass, which can be optimized by modulating the glass composition. The Bi^0 and Bi^+ ions were the NIR luminescence source of the glass samples in this paper. The Bi/Sn-doped aluminosilicate glass has the potential to become a new type of core fiber material and to be applied to optical fiber amplifiers (OFAs), based on its excellent performance in ultra-broadband NIR emission.

Keywords: bismuth; tin; near-infrared; silicate; glass; aluminum

check for updates

Citation: Xiang, S.; Zhang, M.; Zeng, T.; Chen, J.; Zhang, F. Optimizing Broadband Near-Infrared Emission in Bi/Sn-Doped Aluminosilicate Glass by Modulating Glass Composition. *Micromachines* **2022**, *13*, 921. https://doi.org/10.3390/mi13060921

Academic Editor: Giancarlo C. Righini

Received: 16 May 2022
Accepted: 8 June 2022
Published: 10 June 2022

Publisher's Note: MDPI stays neutral with regard to jurisdictional claims in published maps and institutional affiliations.

Copyright: © 2022 by the authors. Licensee MDPI, Basel, Switzerland. This article is an open access article distributed under the terms and conditions of the Creative Commons Attribution (CC BY) license (https://creativecommons.org/licenses/by/4.0/).

1. Introduction

The NIR emission of Bi-doped silica glass in the optical communication window was discovered coincidentally in 1999 by Murata et al. [1]. Fujimoto et al. [2–4] Demonstrated, for the first time, the optical amplification of Bi-doped silica glass at 1.3 μm, which indicates the great potential of this mysterious material for applications in photonic devices. In 2005, Dianov et al. [5] made a breakthrough in bismuth-doped quartz fiber and successfully revealed the first continuous-wave (CW) laser from 1150 to 1300 nm. This implied that the greatest strength of Bi-doped glasses used for optical fiber amplifiers is the optical bandwidth, which cannot be achieved by any rare-earth-doped glass [6–11]. Bi-doped silica glass could be a candidate for a new fiber core material, due to its broadband NIR emission that can cover the low-loss window of quartz fiber [12]. Bi doping broadens the data transmission bandwidth of fiber-optic amplifiers and effectively improves the data transmission capability of fiber-optic systems.

A series of studies focused on the relationship between the components of the bismuth glass and the NIR luminous nature of Bi-doped silica glasses [13–20]. It was found that aluminum doping has a significant effect on the near-infrared luminescence of bismuth and the fluorescence properties of alumina-doped silica glass [13]. A series of Bi-doped germanium-borate glasses had been prepared via a melt–quenching method by Liu X et al. The dual-modulating modes of visible (380~750 nm) and near-infrared (1000~1600 nm) broadband photoemission were effectively controlled with the flexible excitation scheme [14]. Bi-doped nitrogen-germanium acid glass fibers were drained at 900 °C, which increased the spectral bandwidth of Bi-doped optical emitters to >600 nm [15]. It was reported that Sn doping can improve the sensitivity, refractive index, and stability of erbium silica glass by

Chiodini et al. [16]. Numerous experiments confirmed that the NIR luminous properties can be optimized by modulating the content of Bi, Al and Sn. However, the effect of Sn doping on the NIR luminescence properties of the glass is still unclear.

In this study, we selected $64SiO_2$-$5Al_2O_3$-30CaO-$1Bi_2O_3$ as the glass matrix [21–24] to investigate the NIR luminous properties of the Bi/Sn co-mixed aluminosilicate glass system, and analyzed the NIR luminous mechanism of Bi-doped glass. The glass samples were prepared using the melting–quenching method, tested, and analyzed by absorption spectra, NIR emission spectra, and Fourier transform infrared (FTIR) spectra.

2. Experiments

The SiO_2-CaO-Al_2O_3-Bi_2O_3-SnO_2 glass samples were prepared using the traditional melting–quenching method. SiO_2, Al_2O_3, SnO_2, $CaCO_3$, and Bi_2O_3 with high purity (99.99%) were used as starting materials. The raw material was weighed according to the molar ratio, mixed in an agate mortar, then melted in a corundum crucible at 1600 °C for 1.5 h. The melts were subsequently poured onto a cold stainless steel plate, then quickly pressed using another stainless steel plate, which ensured high cooling rates and avoided the possibility of the Bi metal separating out from the glasses, and then they were annealed at 750 °C for 5 h, in order to remove internal stresses. The oval-shaped glass samples were divided into regular squares with side length of 10 mm, and were polished on both the top and bottom surfaces in preparation for optical characterization.

Absorption spectra were recorded by a UV-VIS-NIR spectrophotometer (3600plus, Shimadzu, Japan) and detected by an InGaAs detector. NIR emission spectra were measured on a steady-state fluorescence spectroscopy spectrometer (FLS980, Edinburgh Instruments, EI, Edinburgh, Britain) with 480 nm continuous wave (CW) as the excitation source, and were detected in the range 800–1700 nm. Fourier transform infrared (FTIR) spectra were collected on a Nicolet 6700 FTIR spectrometer (Nicolet, Thermo Fisher Scientific, Waltham, MA, USA) by dispersing glass powders into KBr pellets. X-ray diffraction spectroscopy of the glass samples was recorded using a TD-3500 electronic material structure analyzer at 30 kV/40 mA, Cu/Kα, 2θ range of 5–70°. Solid-state NMR measurements of the sample were conducted at 14.01 T using a JNM-ECZ600R spectrometer (JEOL RESONANCE Inc., Tokyo, Japan) operating at a 1H resonance frequency of 599.7 MHz.

3. Results and Discussion

The absorption spectra of (69-x) SiO_2-xAl_2O_3-30CaO-$1Bi_2O_3$ (x = 5, 10, 15, 20, 25, 30) glass samples are shown in Figure 1a. Two absorption bands were observed at 480 nm and 712 nm, which are similar to the characteristic Bi-related absorption bands observed in various glasses [7,25,26]. Both of them exhibited transmittance of about 88% in the range from 800 nm to 1200 nm. The absorbance at both 480 nm and 712 nm increased with increasing Al_2O_3 concentration at first and then reached a maximum at about 10 mol% Al_2O_3. With the further increase in Al_2O_3 concentration, the absorption peak at 712 nm weakened and disappeared. As compared to the spectroscopic data of both Bi^0 and Bi^+ in previous literature [27,28], the strongest absorption at 480 nm is assigned to the transition of $^4S_{3/2} \rightarrow {}^2P_{1/2}$ of Bi^0, and the absorption at 712 nm is mainly from the transition of $^3P_0 \rightarrow {}^3P_2$ of Bi^+. The photoluminescence (PL) spectra of the glass samples are presented in Figure 1b. A broadband emission at about 1215 nm, with an FWHM of more than 250 nm, could be observed in the NIR PL spectra of the 10Al sample. The intensity of the NIR emission increases first and then decreases with increasing Al_2O_3 concentration. It is well known that Al^{3+} is usually used as a glass modifier or network modifier, which facilitates the formation of Bi NIR centers in Bi-doped silica glass [29,30]. However, the NIR emission characteristics of the glass samples are not monotonically enhanced with increasing Al_2O_3 concentration. The possible reason for this result is the distribution of aluminum in the glass network [30]. The network structure of the glass would be disrupted because of superfluous Al_2O_3 concentration. The increase in four-coordinated tetrahedron sites (AlO_4) in the glass network will weaken the crystal field strength around the bismuth and eventually result in

blue shifts in the NIR emission [31]. The dependencies of emission intensity at 1215 nm with absorbance at 480 nm on Al_2O_3 concentration are shown in Figure 1c. The absorbance and luminescence properties of the glass samples changed significantly with the increase in Al_2O_3 concentration. The variation tendency of the emission intensity agrees well with that of the absorption intensity at 480 nm. This predicated that optimizing NIR emission in Bi-doped aluminosilicate glass could be achieved by modulating Al_2O_3 composition in the glass. As shown in Figure 1b, when the concentration of Al_2O_3 reached 10 mol%, the glass sample showed the strongest NIR emission and widest luminous range, so the amount of Al_2O_3 was 10 mol% in the optimized glass composition. The optimized glass formulation was $59SiO_2$-$10Al_2O_3$-$30CaO$-$1Bi_2O_3$. The appearance of glass samples was affected by Al_2O_3 concentration, and the color gradually became lighter than pink as the Al_2O_3 concentration increased, as shown in Figure 1d.

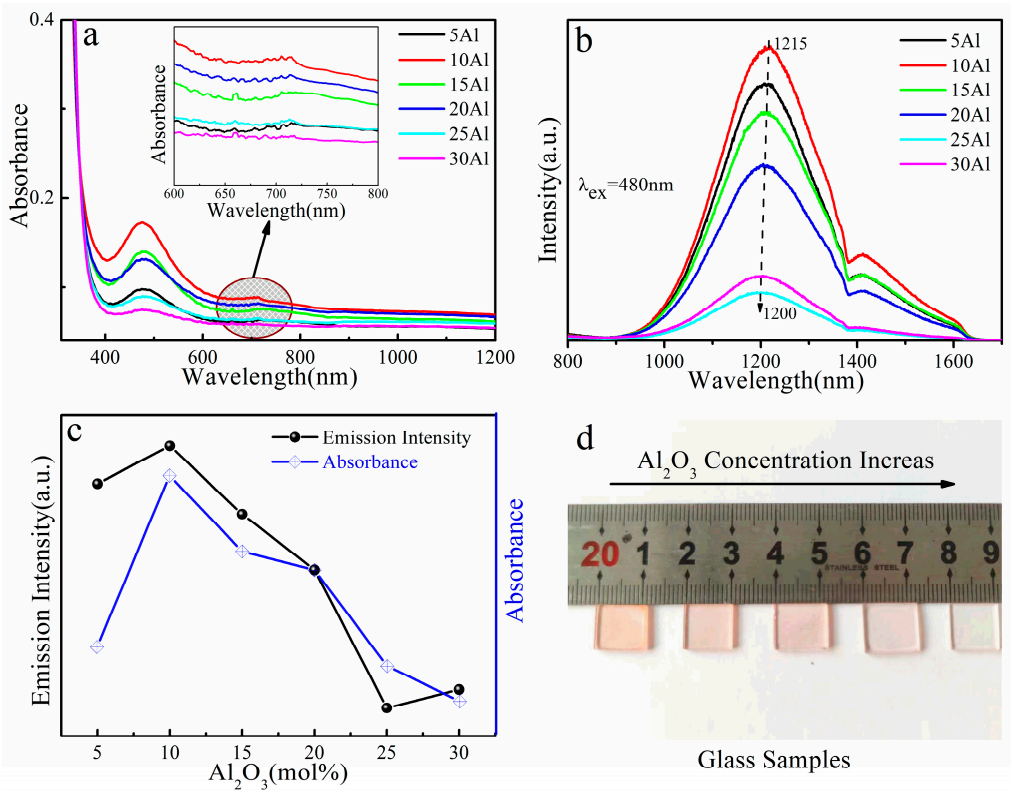

Figure 1. (**a**) Transmission spectra of (69-x) SiO_2-$30CaO$-xAl_2O_3-$1Bi_2O_3$ glasses. The inset shows their transmission spectra in the range from 600 nm to 800 nm. (**b**) PL spectra of (69-x) SiO_2-$30CaO$-xAl_2O_3-$1Bi_2O_3$ glass samples excited by a 480 nm LD. (**c**) Dependencies of emission intensity and transmittance on Al_2O_3 concentration. (**d**) The photo of (69-x) SiO_2-$30CaO$-xAl_2O_3-$1Bi_2O_3$ glass samples.

The NIR PL spectra of (60-x) SiO_2-$10Al_2O_3$-$30CaO$-xBi_2O_3 (x = 0.1, 0.5, 1.0, 1.5, 2.0) glass samples are shown in Figure 2a. A broadband emission at about 1208 nm, with FWHM of about 222 nm, was observed in the NIR PL spectra of sample 0.5 Bi. The NIR emission intensity increases first and then decreases with the increase in Bi_2O_3 concentration. As observed in Figure 2b, the red shift of the emission peaks with increasing Bi_2O_3 content. The reason for the decline in emission at high bismuth doping levels was the typical concentration quenching effect caused by cross relaxation between the Bi^0 ions that are closer together [32]. The dependencies of emission intensity and peak wavelength on Bi_2O_3 concentration are shown in Figure 2b. It is found that the NIR emission of the glass samples reaches a maximum when the Bi_2O_3 doping concentration is 0.5 mol%. The optimized composition for NIR emission was $59.5SiO_2$ -$10Al_2O_3$-$30CaO$-$0.5Bi_2O_3$.

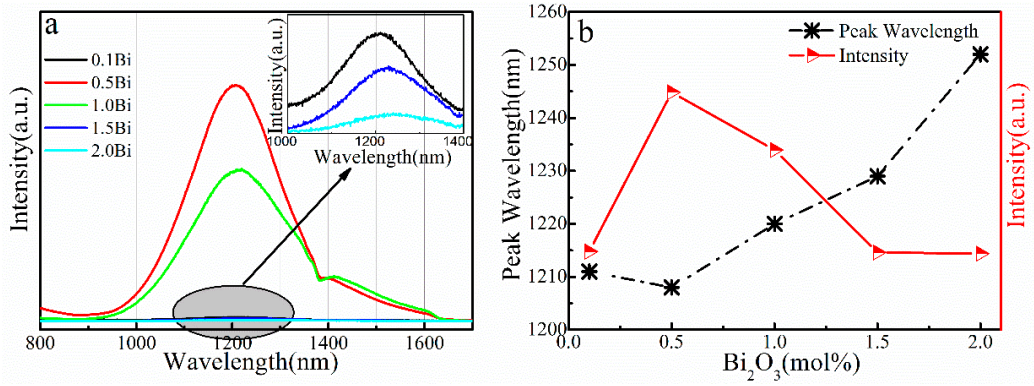

Figure 2. (**a**) PL spectra of glass samples excited by a 480 nm LD. (**b**) Dependencies of emission intensity and peak wavelength on Bi_2O_3 concentration.

The (59.5−x) SiO_2-10Al_2O_3-30CaO-0.5Bi_2O_3-xSnO_2 (x = 0.2, 0.4, 0.6, 0.8, 1.0) glass samples were prepared using the traditional melting–quenching method. Figure 3a indicates the absorption spectra of (59.5−x) SiO_2-10Al_2O_3-30CaO-0.5Bi_2O_3-xSnO_2 glasses. The inset shows the absorbance of glass samples in the range from 400 nm to 600 nm. One main absorption band is observed at about 480 nm. It can be noted that there is no apparent absorption observed around 800 nm, which has been frequently reported in germinate glasses doped with bismuth concentrations higher than 0.5 mol% [26,33]. The intensity of the absorption band at 480 nm is weakest when the SnO_2 concentration reaches 0.8 mol%. There was no significant change in the transparency of the glasses.

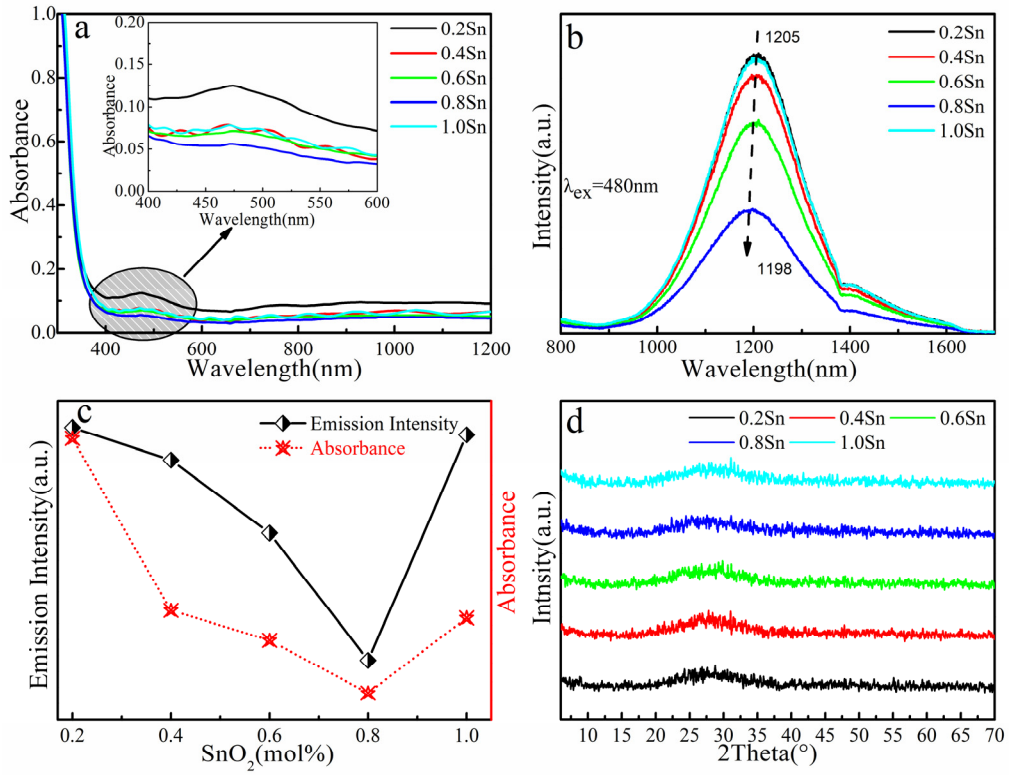

Figure 3. (**a**) Absorption spectra of (59.5-x) SiO_2-10Al_2O_3-30CaO-0.5Bi_2O_3-xSnO_2 (x = 0.2, 0.4, 0.6, 0.8, 1.0) samples. The inset shows their absorbance in the range from 400 nm to 600 nm. (**b**) PL spectra of the (59.5-x) SiO_2-10Al_2O_3-30CaO-0.5Bi_2O_3-xSnO_2 glass samples excited by a 480 nm LD. (**c**) Dependencies of emission intensity and absorption spectra on SnO_2 concentration. (**d**) XRD patterns of the (59.5-x) SiO_2-10Al_2O_3-30CaO-0.5Bi_2O_3-xSnO_2 samples.

The NIR PL spectra of (59.5−x) SiO_2-10Al_2O_3-30CaO-0.5Bi_2O_3-xSnO_2 glasses are shown in Figure 3b, which are measured by introducing an LD at 480 nm with a 75 W Xe900 lamp. An ultra-broadband NIR emission covering 900–1600 nm is observed in all samples. When the SnO_2 concentration was increased to 0.8 mol%, the intensity of the NIR emission reached a minimum and then enhanced with increasing SnO_2 concentration. We estimate that the blue shift of Bi NIR emission is due to the loss of low-valent Bi ions. The dependencies of emission intensity at 1206 nm with absorbance at 480 nm on SnO_2 concentration are shown in Figure 3c; with the increase in SnO_2 concentration, the absorption and luminescence properties of the glass samples indicate the same trend of change. Figures 1c and 3c indicate that the absorption and luminescence properties of the Bi-doped glasses depend on the glass composition. Therefore, the optimized NIR PL nature of Bi/Sn-doped glass could be achieved by Bi/Sn co-mixed composition. The final optimized composition for NIR emission is 58.5SiO_2–10Al_2O_3– 30CaO–0.5Bi_2O_3–1SnO_2. Figure 3d illustrates the X-ray diffraction spectroscopy. The peak in the 25–30° range was a typical glass diffusion peak. No diffraction peak was observed, proving the amorphous state of the samples. The result of XRD indicated that the addition of SnO_2 did not change the phase of the glass samples.

The luminescence properties of Bi-doped silica glass depend on the valence state of Bi. The valence of bismuth in glass is easily influenced by the surrounding environment, such as the concentration of non-bridging oxygens (NBOs) in the glass. The FTIR spectra can directly show the existence of NBOs. To understand the nature of the changes in NIR luminescence in glass samples, the FTIR spectra were measured. The FTIR spectra of (59.5-x) SiO_2-10Al_2O_3-30CaO-0.5Bi_2O_3-xSnO_2 glass samples are illustrated in Figure 4a. Five noticeable peaks of glass samples could be traced at ~1192, ~1047, ~985, ~714 and ~463 cm^{-1} in the FTIR spectra. The peaks at ~1192 and ~1047 cm^{-1} were Si-O-Si asymmetrical stretching vibrations. The asymmetric stretching vibration peak of the terminal Si-O bonds is at ~985 cm^{-1}. The relative intensity of the vibration peak at ~985 cm^{-1} is decreases with the increase in SnO_2 concentration, up to 0.8 mol%, and then increases with the further increase in SnO_2 concentration, indicating that the amount of NBOs is changed and the glass is depolymerized. In addition, during the depolymerization of glass network, Si-O-Al bonds were preferentially broken down due to their longer bond length than Si-O-Si [22]. The Al-O stretching vibrations in isolated AlO_4 (~714 cm^{-1}) are decreased when more SnO_2 is incorporated into the silica network. To support the result of the FTIR spectra, the ^{27}Al NMR spectra of (59.5-x) SiO_2-10Al_2O_3-30CaO-0.5Bi_2O_3-xSnO_2 glass samples are collected, as shown in Figure 4b. Vast majority of the aluminum exists in AlO_4 (60ppm), and the change in AlO_4 coincides with the change in the FTIR spectra. AlO_4 favors the existence of lower-valence-stated bismuth and enhances its NIR emission [31], and NBOs would reduce its NIR emission. As shown in Figure 3b, the NIR emission decreases at first and then increases with the concentration of SnO_2; this is caused by the competitive effect of NBOs and AlO_4.

There is still controversy about the NIR luminescence of Bi-doped silica glass, which has mainly been attributed to higher-valent Bi, such as Bi^{5+} [3], and lower-valent Bi, such as Bi^+ [21] and Bi^0 [7]. Qiu, J et al. [7] reported that when excited by 610 nm light, Bi^+ and Bi^0 are excited, but the $^2P_{1/2} \rightarrow {}^4S_{3/2}$ transition of Bi^0 plays a dominant role, resulting in an emission band at 1210 nm. According to the research of Liu, X et al. [14], excitation at either 460 or 780 nm always produces broad emissions in the NIR region of 1000~1600 nm, which corresponds to the transition of $^2D_{3/2} \rightarrow {}^4S_{3/2}$ of Bi^0 and the transition of $^3P_1 \rightarrow {}^3P_0$ of Bi^+, respectively. Combined with the spectral data (shown in Figures 1b and 3b), the NIR luminous bands were around 1205 nm for all the glass samples. We suggested that both the Bi^0 and Bi^+ active centers may exist in our glass samples. Further assignments will be discussed.

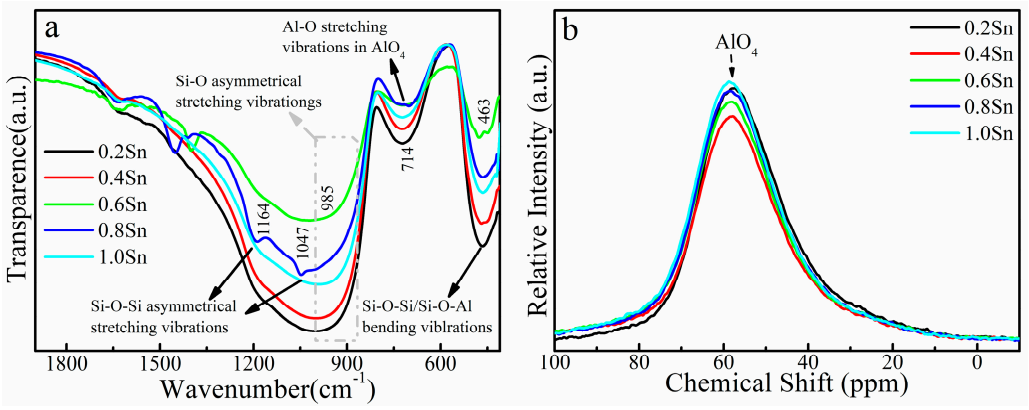

Figure 4. (**a**) FTIR spectra of 59.5SiO_2-10Al_2O_3-30CaO-0.5Bi_2O_3-xSnO_2 glass samples. (**b**) ^{27}Al NMR spectra of (59.5-x) SiO_2-10Al_2O_3-30CaO-0.5Bi_2O_3-xSnO_2 glass samples.

In general, the absorption edge is caused by the electronic transitions, which also reflects the optical band gap of materials. As developed by Tauc and Menth [34], the absorption coefficient *(α)* obeys the following relation for most amorphous materials:

$$(\alpha h\upsilon)^n = B(h\upsilon - E_g) \quad (1)$$

Here, α is the absorption coefficient, and α can be obtained from the transmittance T and thickness d of the glass ($\alpha = -\lg T/d$); $h\upsilon$ is the incident photon energy; B is an energy-independent constant; Eg is the band gap energy; and n is the nature of transition. By plotting $(\alpha h\upsilon)^n$ as a function of $h\upsilon$ (Tauc's plot), one can find the optical band gap. Finally, values of Eg are determined from the extrapolation of the linear region of $(\alpha h\upsilon)^n = 0$ and are listed in Table 1. It was seen that the optical band gap decreased slightly with the SnO_2-doped glass sample, corresponding to the progressive red shift of the absorption edge [14]. We empirically attributed this decrease in the band gap (or red shift of the absorption edge) to the reduction in the relative content of Bi^0; that is, more introduced SnO_2 was converted into higher-valent Bi species in the glass samples, leading to a decrease in Bi^0 absorption (shown in Figures 1a and 3a). Meanwhile, the NIR luminescence intensity of the glass samples also decreased. The NIR luminescence center of Bi-doped glass stemming from low-valent Bi^0 and Bi^+ was confirmed.

Table 1. Optical band gap of the glasses.

xAl Sample	Eg ± 0.01 (eV)	xSn Sample	Eg ± 0.01 (eV)
5Al	3.83	0.2Sn	3.76
10Al	3.87	0.4Sn	3.77
15Al	3.85	0.6Sn	3.79
20Al	3.84	0.8Sn	3.77
25Al	3.82	1.0Sn	3.72
30Al	3.81		

4. Conclusions

To sum up, the influence of the concentration of aluminum and bismuth on the NIR emission properties of silica glass, based on the 64SiO_2-5Al_2O_3-30CaO-1Bi_2O_3 glass composition, was studied separately, and then the effects of co-mixed Bi/Sn on the NIR luminescence properties of glass were investigated. According to the spectral data, we found that the NIR emission intensity has a certain dependence on the components of Bi/Sn-doped glasses. When the concentrations of Al_2O_3, Bi_2O_3, and SnO_2 were 10, 0.5, and 1.0 mol%, respectively, the glass samples had the strongest NIR luminescence intensity, as shown in Figures 1b, 2a and 3b. A broadband emission at about 1206 nm, with FWHM of more than 220 nm, can be observed in the NIR PL spectra of the glass samples. The optimal

formulation for NIR emission is 58.5SiO_2-10Al_2O_3-30CaO-0.5Bi_2O_3-1.0SnO_2 (mol%). It is considered that the Bi^0 and Bi^+ were the NIR luminescence source of the glass samples in this thesis. The study on the luminescence center of bismuth-doped glasses indicated that SnO_2 doping reduces the low-valent Bi ion concentration, which reduces the NIR luminescence intensity of the glass. Tunable NIR emission was observed by changing the glass components. The present investigation will be of value for designing suitable glass composition.

Author Contributions: Conceptualization, M.Z.; methodology, S.X. and M.Z.; investigation, S.X.; resources, M.Z., T.Z., J.C. and F.Z.; data curation, S.X. and J.C.; writing—original draft preparation, S.X.; writing—review and editing, M.Z.; supervision, M.Z.; project administration, M.Z., T.Z. and F.Z.; funding acquisition, M.Z., T.Z. and F.Z. All authors have read and agreed to the published version of the manuscript.

Funding: The research was supported by the National Natural Science Foundation of China (Grant No.11804281). Nanchong Science and Technology Project (Grant No.21GXJS0014).

Conflicts of Interest: The authors declare no conflict of interest.

References

1. Murata, K.; Fujimoto, Y.; Kanabe, T. Bi-Doped SiO2 as a New Laser Material for an Intense Laser. *Fusion Eng. Des.* **1999**, *44*, 437–439. [CrossRef]
2. Fujimoto, Y.; Nakatsuka, M. Optical amplification in bismuth-doped silica glass. *Appl. Phys. Lett.* **2003**, *82*, 3325–3326. [CrossRef]
3. Fujimoto, Y.; Nakatsuka, M. Infrared luminescence from bismuth-doped silica glass. *Jpn. J. Appl. Phys.* **2001**, *40*, L279. [CrossRef]
4. Fujimoto, Y.; Matsubara, H.; Nakatsuka, M. New fluorescence from Bi-doped silica glass and its 1.3-/spl mu/m emission with 0.8-/spl mu/m excitation for fiber amplifier. In Proceedings of the Technical Digest. CLEO/Pacific Rim 2001. 4th Pacific Rim Conference on Lasers and Electro-Optics (Cat. No.01TH8557), Chiba, Japan, 15–19 July 2001; Volume 2, p. II.
5. Dianov, E.M.; Dvoyrin, V.V.; Mashinsky, V.M. CW bismuth fibre laser. *Quantum Electron.* **2005**, *35*, 1083. [CrossRef]
6. Liang, H.; Wang, X.; Yu, J.; Yang, W.; Lewis, E.; Wang, P. Bismuth-doped compound germanate glass microsphere lasing in the near-infrared region. *Microw. Opt. Technol. Lett.* **2020**, *62*, 67–71. [CrossRef]
7. Zhang, N.; Qiu, J.; Dong, G.; Yang, Z.; Zhang, Q.; Peng, M. Broadband tunable near-infrared emission of Bi-doped composite germanosilicate glasses. *J. Mater. Chem.* **2012**, *22*, 3154–3159. [CrossRef]
8. Dianov, E.M. Bi-doped optical fibers: A new active medium for NIR lasers and amplifiers. In Proceedings of the SPIE—The International Society for Optical Engineering, San Jose, CA, USA, 19 January 2008; p. 8601.
9. Chen, D.; Wang, Y.; Bao, F.; Yu, Y. Broadband near-infrared emission from Tm^{3+}/Er^{3+} co-doped nanostructured glass ceramics. *J. Appl. Phys.* **2007**, *101*, 113511. [CrossRef]
10. Afef, B.; Alqahtani, M.M.; Hegazy, H.H.; Yousef, E.; Damak, K.; Maâlej, R. Green and near infrared emission of Er^{3+} doped PZS and PZC glasses. *J. Lumin.* **2018**, *194*, 706–712. [CrossRef]
11. Liu, J.; Huang, X.; Pan, H.; Zhang, X.; Fang, X.; Li, W.; Xiao, Z. Broadband near infrared emission of Er^{3+}/Yb^{3+} co-doped fluorotellurite glass. *J. Alloy. Compd.* **2021**, *866*, 158568. [CrossRef]
12. Alsingery, R.M.; Mudhafer, A. Development of Bismuth-Doped Fibers (BDFs) in Optical Communication Systems. In *Bismuth-Fundamentals and Optoelectronic Applications*; IntechOpen: London, UK, 2020.
13. Fujimoto, Y.; Nakatsuka, M. 27Al NMR structural study on aluminum coordination state in bismuth doped silica glass. *J. Non-Cryst. Solids* **2006**, *352*, 2254–2258. [CrossRef]
14. Liu, X.; Cheng, C.; Li, X.; Jiao, Q.; Dai, S. Controllable ultra-broadband visible and near-infrared photoemissions in Bi-doped germanium-borate glasses. *J. Am. Ceram. Soc.* **2020**, *103*, 183–192. [CrossRef]
15. Cao, J.; Wondraczek, L.; Wang, Y.; Wang, L.; Li, J.; Xu, S.; Peng, M. Ultrabroadband near-infrared photoemission from bismuth-centers in nitridated oxide glasses and optical fiber. *Acs Photonics* **2018**, *5*, 4393–4401. [CrossRef]
16. Chiodini, N.; Paleari, A.; Spinolo, G.; Chiasera, A.; Ferrari, M.; Brambilla, G.; Taylor, E.R. Photosensitive erbium doped tin-silicate glass. *J. Non-Cryst. Solids* **2002**, *311*, 217–222. [CrossRef]
17. Peng, M.; Qiu, J.; Chen, D.; Meng, X.; Zhu, C. Superbroadband 1310 nm emission from bismuth and tantalum codoped germanium oxide glasses. *Opt. Lett.* **2005**, *30*, 2433–2435. [CrossRef] [PubMed]
18. Qiu, J.; Peng, M.; Ren, J.; Meng, X.; Jiang, X.; Zhu, C. Novel Bi-doped glasses for broadband optical amplification. *J. Non-Cryst. Solids* **2008**, *354*, 1235–1239. [CrossRef]
19. Li, X.; Cao, J.; Huang, M.; Peng, M. Modulating broadband near infrared emission from Bi doped borate laser glass by codoping nonactive rare earth ions. *J. Non-Cryst. Solids* **2021**, *553*, 120477. [CrossRef]
20. Meng, X.G.; Qiu, J.R.; Peng, M.Y.; Chen, D.P.; Zhao, Q.Z.; Jiang, X.W.; Zhu, C.S. Infrared broadband emission of bismuth-doped barium-aluminum-borate glasses. *Opt. Express* **2005**, *13*, 1635–1642. [CrossRef]

21. Zhou, S.; Feng, G.; Bao, J.; Yang, H.; Qiu, J. Broadband near-infrared emission from Bi-doped aluminosilicate glasses. *J. Mater. Res.* **2007**, *22*, 1435–1438. [CrossRef]
22. Li, X.; Peng, M.; Cao, J.; Yang, Z.; Xu, S. Distribution and stabilization of bismuth NIR centers in Bi-doped aluminosilicate laser glasses by managing glass network structure. *J. Mater. Chem. C* **2018**, *6*, 7814–7821. [CrossRef]
23. Suzuki, T.; Ohishi, Y. Ultrabroadband near-infrared emission from Bi-doped Li2O-Al2O3-SiO2 glass. *Appl. Phys. Lett.* **2006**, *88*, 191912. [CrossRef]
24. Li, X.; Cao, J.; Wang, L.; Peng, M. Predictable tendency of Bi NIR emission in Bi-doped magnesium aluminosilicate laser glasses. *J. Am. Ceram. Soc.* **2018**, *101*, 1159–1168. [CrossRef]
25. Dianov, E.M. Amplification in extended transmission bands using bismuth-doped optical fibers. *J. Lightwave Technol.* **2012**, *31*, 681–688. [CrossRef]
26. Meng, X.G.; Qiu, J.R.; Peng, M.Y.; Chen, D.P.; Zhu, C.S. Near infrared broadband emission of bismuth-doped aluminophosphate glass. *Opt. Express* **2005**, *13*, 1628–1634. [CrossRef] [PubMed]
27. Zheng, J.Y.; Tan, L.N.; Wang, L.P.; Peng, M.Y.; Xu, S.H. Superbroad visible to NIR photoluminescence from Bi^{+} evidenced in $Ba_2B_5O_9Cl$: Bi crystal. *Opt. Express* **2016**, *24*, 2830–2835. [CrossRef]
28. Romanov, A.N.; Veber, A.A.; Fattakhova, Z.T.; Vtyurina, D.N.; Kouznetsov, M.S.; Zaramenskikh, K.S. Spectral properties and NIR photoluminescence of Bi^{+} impurity in $CsCdCl_3$ ternary chloride. *Lumin* **2014**, *149*, 292–296. [CrossRef]
29. Doweidar, H. Density-structure correlations in Na2O-Al2O3-SiO2 glasses. *J. Non-Cryst. Solids* **1998**, *240*, 55–65. [CrossRef]
30. Abd El-Moneim, A.; Youssof, I.M.; El-Latif, L.A. Structural role of RO and Al2O3 in borate glasses using an ultrasonic technique. *Acta Mater.* **2006**, *54*, 3811–3819. [CrossRef]
31. Li, X.; Cao, J.; Peng, M. The origin of the heterogeneous distribution of bismuth in aluminosilicate laser glasses. *J. Am. Ceram. Soc.* **2018**, *101*, 2921–2929. [CrossRef]
32. Qian, M.; Cheng, J.; Hu, L. Dependence of spectroscopic properties on doping content and temperature of bismuth-doped lanthanum aluminosilicate glass. *Chin. Opt. Lett.* **2012**, *10*, 111602. [CrossRef]
33. Cl, A.; Yz, B.; Jha, C.; Jian, R.; Chao, L.; Xza, C. Multi-band near-infrared emission in low concentration bismuth doped alkaline earth alumino-boro-germanate glass-sciencedirect. *Ceram. Int.* **2020**, *46*, 15544–15553.
34. Zhang, Q.Y.; Zhang, W.J.; Wang, W.C.; Jiang, Z.H. Calculation of physical properties of glass via the phase diagram approach. *Non-Cryst. Solids* **2017**, *457*, 36–43. [CrossRef]